

Integrated Setup for THz Receiver Characterization

O. Nyström^{1,*}, H. Rashid¹, B. Billade¹, E. Sundin¹, M. Fredrixson¹, G. Johnsen¹, I. Lapkin¹, D. Meledin¹, M. Strandberg¹, R. Finger², A. Pavolotsky¹, V. Desmaris¹, and V. Belitsky¹

¹*Chalmers University of Technology, Group of Advanced Receiver Technology, Gothenburg, SWEDEN*

²*University of Chile, Santiago, CHILE*

*Contact: olle.nystrom@chalmers.se, phone +46-31-772 1838

Abstract — A highly versatile measurement setup has been built that allows complete characterization of the ALMA Band 5 cartridge. The measurement setup includes all necessary hardware and largely achieves automatic measurements for the system noise and sideband rejection with in-built optimization procedures. The measurement setup additionally comprises measurements of the receiver saturation, phase and amplitude stability, as well as optical beam characterization.

I. INTRODUCTION

The Atacama Large Millimeter/sub-millimeter Array (ALMA) is a partnership of Europe, Japan, and North America, in cooperation with the Republic of Chile. ALMA will initially be composed of 66 high-precision antennas with a possible extension in the future [1]. The ALMA site is located at an altitude of 5000 m in the Atacama desert in northern Chile.

The ALMA Band 5 receiver channel is a dual polarization, sideband separation (2SB) SIS-receiver [2] and covers the frequency range 163-211 GHz that includes the 183 GHz water absorption line. The presence of the water absorption line in the receiver RF band makes ground based observations challenging. However, the scientific drive for the development of the ALMA Band 5 cartridge is to observe the water line in space whereas the extremely dry, high-altitude site in the Atacama desert allows observations even at these frequencies. Apart from observing the water, the second drive for the Band 5 development is to detect highly red shifted galaxies, which falls in the specified frequency range [3].

The presence of the strong absorption line within ALMA B5 RF- band implies additional challenges in the receiver characterization, since the water vapour introduces substantial RF - loss affecting the accuracy of the measurements. The ALMA B5 characterization takes place in the laboratory in Gothenburg, Sweden, located at sea level, with a typical humidity of 70-90 % [4]. In order to preclude the humidity to affect the accuracy of the measurements, the RF-part of the setup is enclosed in a cabinet, constantly flushed with dry nitrogen. The enclosing of the measurement setup requires a highly compact layout, which was realized using a layered design. The layout of the measurement setup is described in section II. Section III-V of this paper describes different parts of the measurement setup, i.e. noise/sideband-rejection measurements and optimization, gain saturation, phase-stability, and optical characterization.

II. MEASUREMENT SETUP LAYOUT

The measurement setup has been built with focus to be compact and to allow largely automatic measurements and optimization of the receiver performance of the ALMA B5 Cartridge. The 183 GHz water absorption line is situated in the middle of the receiver's RF - band and introduces substantial RF - loss affecting the accuracy of the measurements. Consequently, the RF-part of the setup is enclosed inside a cabinet, which is constantly flushed with dry nitrogen in order to minimize the effect of the water vapour on the accuracy of the measurements. The layout of the measurement setup is shown in Fig. 1.

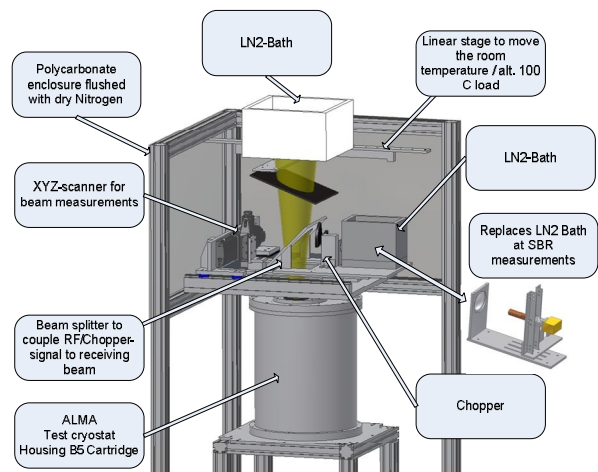


Fig. 1 Layout of measurement setup used for ALMA B5 cartridge characterization. The scanner, CW-source, and the hot/cold loads are placed in "layers" above the RF window allowing a compact setup and, to a large extent, automatic measurements.

Reduction of the water vapour in the enclosure allows the cold (77 K) LN2 load to be placed above the cryostat window at a sufficient distance to facilitate the use of hot loads: 290 K for the noise measurement setup (Y-factor measurements) and 373 K load for the dynamic range characterization, which are located in between the cryostat window and the cold load. Appropriate loads for the different measurements are inserted with computer controlled linear stages. The top plate of the cryostat accommodates the beam scanner for optical characterization that is placed in the "layer" below the loads. The use of computer controlled linear stages allows easy reconfiguration of the setup for different type of measurements.

III. NOISE AND SIDEBAND REJECTION MEASUREMENTS

We use standard Y-factor measurement technique where the receiver input is either exposed to 77 K load, the load being manufactured as described in [5] and immersed into liquid nitrogen, or to a hot load. A Mylar beam-splitter is used to inject the CW test signal in the main beam with background loaded to the cold facility load while performing the noise and sideband rejection (SBR) tuning of the receiver. The hot (room temperature) load is inserted into the receiver beam by a computer controlled linear stage; this allows simultaneous measurements and optimization for sideband rejection and noise temperature. The optimization routine finds the optimum settings with the LO-control voltage (LO-power) and the mixer bias settings as variables.

The Mylar beam-splitter (at 300 K) introduces some, but insignificant loss in the cold load signal path; our estimation predicts that the effective load temperature should not exceed 90 K and is corrected through calibration. By performing the sideband rejection measurements with a CW pilot signal with a background of approximately 90 K, we minimize potential problems with the SIS mixer saturation. The sideband rejection measurement follows the approach proposed in [6]. Fig. 2 shows a picture of the setup in SBR configuration.

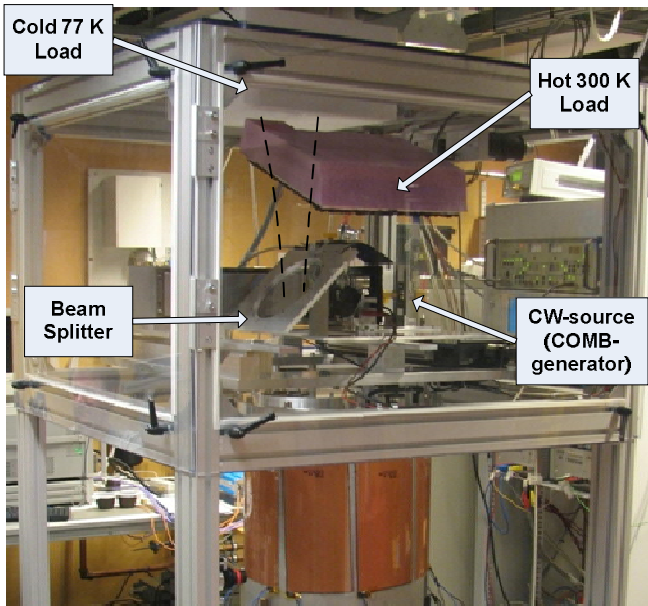


Fig. 2 Measurement setup in configuration for noise and sideband rejection measurement and optimization.

IV. GAIN SATURATION MEASUREMENTS

SIS-mixers are selected as detectors for receivers in radio-astronomy due to their extremely high sensitivity, resulting from high non-linear behavior (non-linear at voltages in the order of 1mV). A drawback of this behavior is that a SIS-mixer might saturate at input power levels from blackbody radiation at temperatures just above room temperature. The ALMA specifications require that the large signal gain compression shall be less than 5 % measured with 77 K load at the RF input port and the situation when a 373 K load is placed at the same RF input port [7].

Reference [8] outlined how the large signal gain compression, GC_{ls} , between two input levels can be determined by measuring the differential gain at the same input levels. Fig. 3 and Fig.4, from [8], illustrate how the large signal gain compression and the differential gain are defined; 1) T_{sys} (Receiver temperature + T_{in}) vs. P_{out} and 2) T_{in} vs. P_{out} . The large signal gain compression is defined as G_0/G_1 and the differential gain is defined as dP_{out}/dP_{in} . Further, [8] shows that; 1) the large signal gain is different (due to the redefinition of the origin); 2) the differential gains and gain compression is the same; 3) the large signal gain compression has the same value; 4) $GC_{ls} = \frac{1}{2} GC_{diff}$.

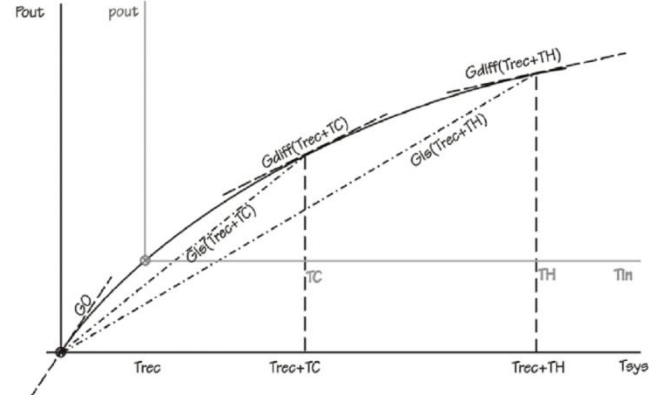


Fig. 3 The large-signal and differential gain is illustrated at two different input temperatures at the input of the receiver (P_{out} vs. T_{sys}). The input considered is $T_{rec}+T_{in}$, i.e. T_{sys} [8].

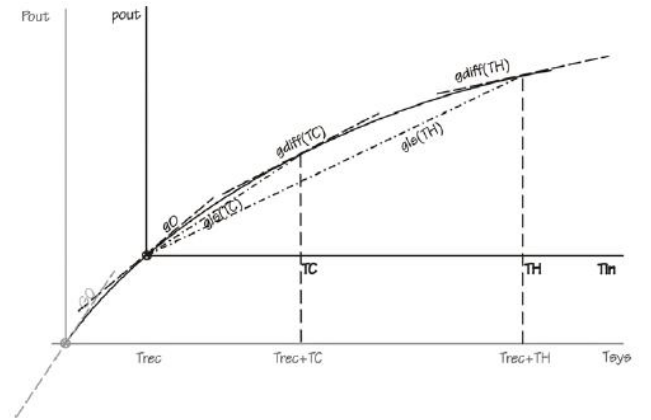


Fig. 4 The large-signal and differential gain is illustrated at two different input temperatures at the input of the receiver (P_{out} vs. T_{in}). The input considered is T_{in} only [7].

In our setup, a setup similar to what is presented in [8]; the receiver beam is coupled via the beam-splitter in straight direction to a hot/cold (373K/100K) load to allow alternating the input power between these two levels. The side-beam coupled via the beam-splitter to a signal, which is modulated between the ambient/cold loads by a chopper. This procedure allows measurements of the small signal gain compression at the operating points set by the main hot/cold loads. The principle of the gain saturation setup is shown in Fig. 5 and Fig. 6 shows a picture of the laboratory setup.

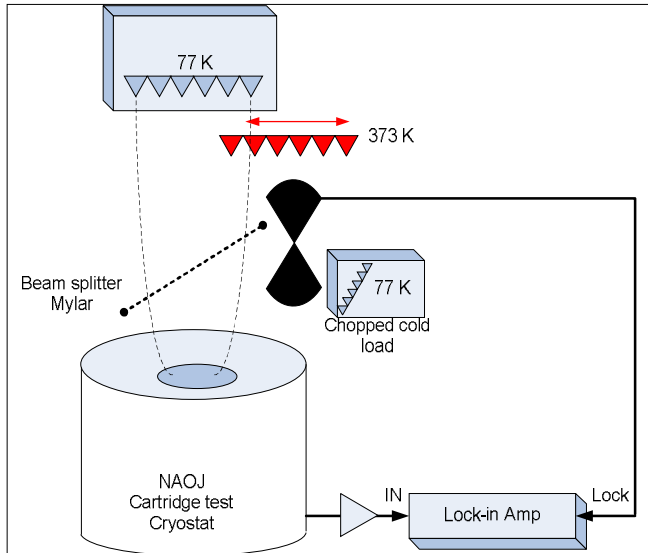


Fig. 5 Layout of gain compression measurement setup. A modulated signal is introduced through beam-splitter allowing measurements of differential gain around operating points set by the main hot/cold loads.

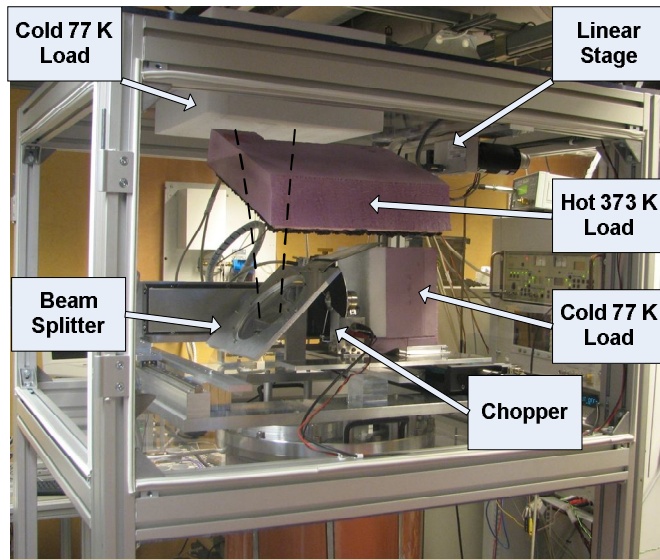


Fig. 6 Picture of the laboratory setup for saturation measurements.

V. BEAM CHARACTERIZATION AND PHASE STABILITY MEASUREMENTS

The receiver optics characterization (beam-pattern measurements) are performed using vector field, both phase and amplitude, measurements. A three axis scanner, allowing compensation for standing waves with its 3rd axis, is used to scan a test RF-source across the receiver input beam. In this setup, a vector network analyser is employed as a single frequency source together with a circuitry, generating necessary frequencies. The circuitry consists of comb-generators, filters, and amplifiers forming a homodyne receiver in order to produce perfectly phase-coherent RF- and LO- signals by taking advantage of different harmonics [9]. The advantage of employing the VNA in combination with the additional circuitry is that such circuitry produces phase

coherent LO and RF signals and removes errors due to initial phase fluctuations in the VNA. The very same setup is also utilized in phase-stability measurements. A schematic of the circuitry is shown in Fig. 7 and a picture of the scanner setup mounted on the cartridge test cryostat is shown in Fig. 8.

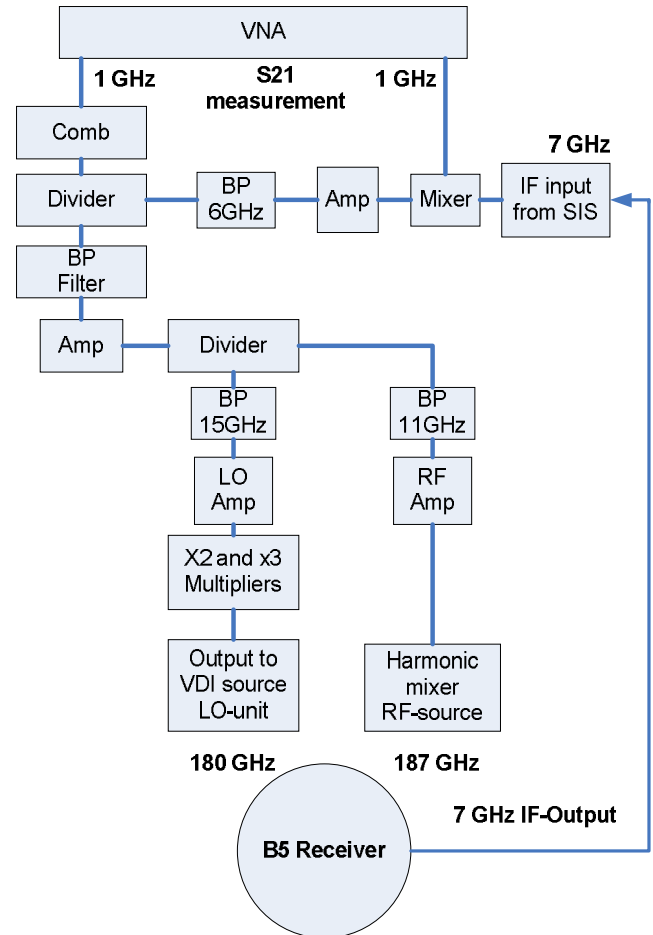


Fig. 7 Schematic of the circuit allowing phase coherent beam scanning. The circuitry is also used in phase stability measurements.

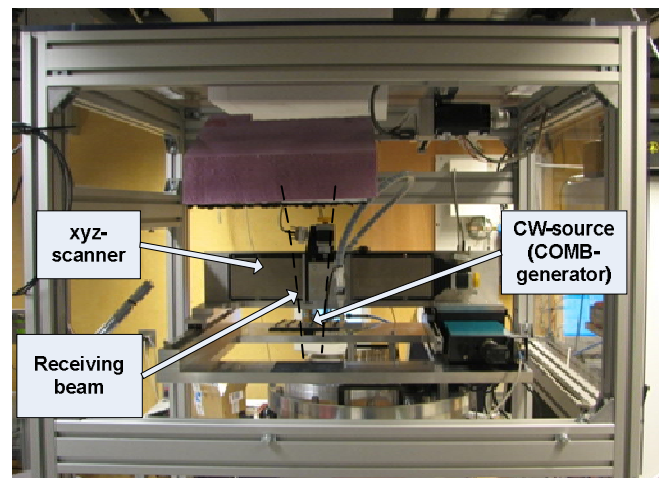


Fig. 8 Picture of the beam scanning setup with the scanner mounted on the cryostat top plate.

Measurements are performed at 168 GHz, 187 GHz, and 210 GHz, thus verifying the optical performance across the frequency band of the receiver. This reflects some limitation of the system in so far as only certain discrete frequencies across the RF – band can be used, since the generated harmonics, producing RF- and LO- signals, must generate an IF signal within the 4-8 GHz range. Figures 9-10 show the measured beam data at 168 GHz.

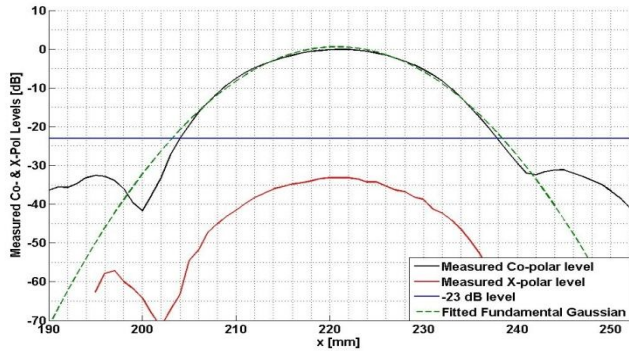


Fig 9 Measured beam, X-cut with Co- and Cross-polar levels in dB, at 168 GHz.

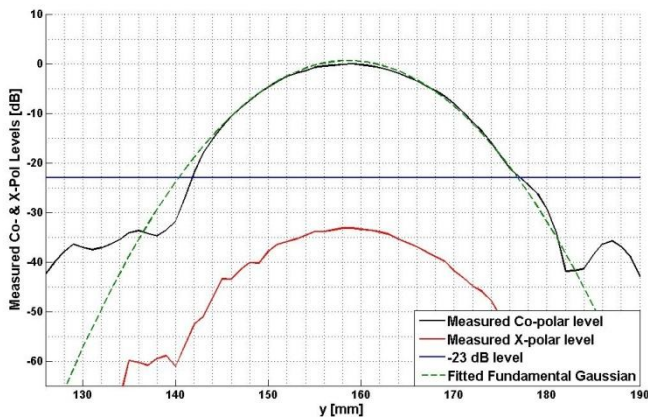


Figure 10 Measured beam, Y-cut with Co- and Cross-polar levels in dB, at 168 GHz.

The measured cross-polarization levels show in Fig 9- Figure 10, exhibit a more Gaussian like shape instead of the characteristic two-lobe shape expected for the cross polar beam pattern. The reason for this is most likely due to a small yaw- angle between the receiving horn and the probe, thus the polarization alignment is not correct and a small part of the co-polar field will be present in the cross-polar pattern. Since the cross polar levels are very low (below -23 dB), compared to the co-polar on axis value, it is sufficient with just a small percentage of the co-polar field to end up with the Gaussian shape of the cross-polar pattern instead of the two lobe pattern. The alignment (yaw-alignment) of the measurement setup will be investigated and the cross polarization will be remeasured.

The beam pattern, horn and mirrors, was previously measured in a room temperature setup using an Agilent VNA with frequency extension modules, results are shown in Fig 11 and Fig 12, where the measured data is displayed together with GRASP [10] and MODAL [11] physical optics

(PO) simulation data. The GRASP and MODAL simulations were performed by M. Whale at NUI Maynooth. The scans are performed at a distance corresponding to the focal plane of the telescope and the measured and simulated data has a correspondence of >99%. The fact that warm optics measurements show nearly 100 % agreement to the simulated data gives confidence that the optics performance is well within specifications and demonstrates the accuracy of the measurements.

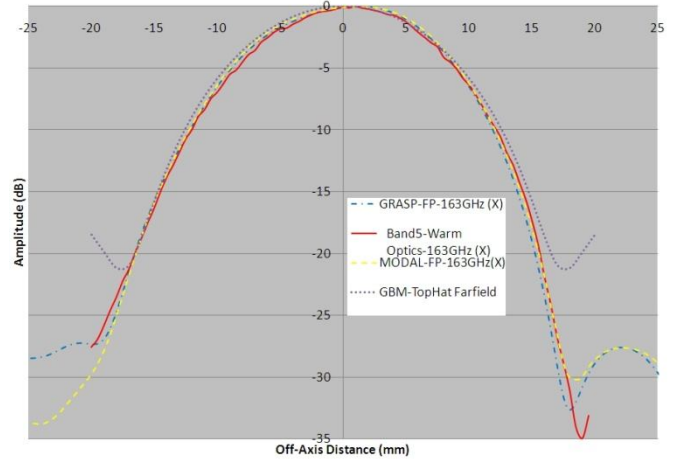


Fig 11 Measured beam pattern, at the focal plane, of the horn and two mirrors at room temperature compared to PO simulations in GRASP and MODAL. The figure shows the x-cut at 163 GHz.

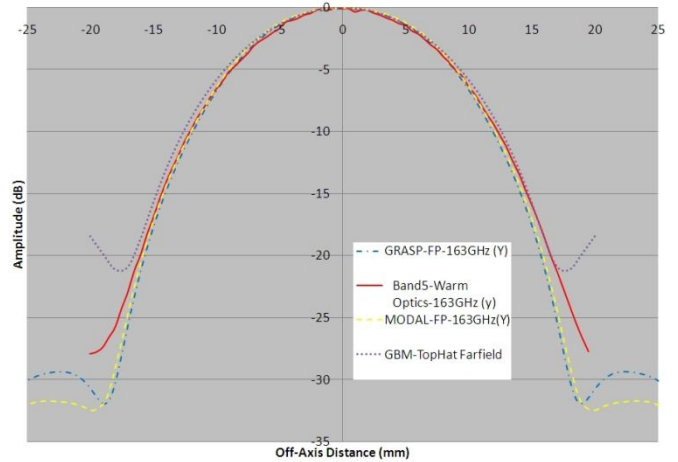


Fig 12 Measured beam pattern, at the focal plane, of the horn and two mirrors at room temperature compared to PO simulations in GRASP and MODAL. The figure shows the y-cut at 163 GHz.

In order to reduce the scan time, which can have a duration exceeding 12 h for dense scans with standing wave compensation, i.e. two measurements $\lambda/4$ apart in z-direction for each point, an on-fly measurement procedure is being implemented. The on-fly measurement reduces the scan time significantly to approximately 40 minutes. The on-fly measurements require high dynamic range and the procedure has been tested successfully with the room temperature setup where the dynamic range of the system is in the order of 80 dB. On-fly measurements will be tested also for cold

measurements for the frequency points where the dynamic range allows. On-fly measurements have the advantage of removing vibrations, due to starts and stops at each point, which otherwise requires a short delay in between measurement samples in order to allow vibrations to decay. The results of the measurements will be compared to the stepped scans for verification.

VI. CONCLUSIONS

We have presented a setup for complete characterization of a 2SB and dual-polarization receiver built in a compact, design. The layered layout, i.e. scanner and loads at different distances along the beam, is used. The entire RF-part of the setup is enclosed in a cabinet flushed with dry nitrogen, reducing the water vapour content and substantial RF-loss compromising the accuracy of the measurements. The presented setup allows largely automated measurements and optimization of the noise and sideband rejection performance of the receiver. By introducing appropriate loads with computer controlled linear stages and applying a CW signal via beam splitter for SBR measurements, Y-factor and sideband rejection measurements can be done simultaneously with significantly decreased time needed for complete receiver characterization.

ACKNOWLEDGMENT

The authors would like to acknowledge Mark Whale, NUI Maynooth for help with PO simulations, Douglas Henke, HIA-NRC (former GARD member) for interesting discussions regarding the layout of the system, and Sven-Erik Ferm for machining excellent mechanical parts.

REFERENCES

- [1] ALMA Observatory Website, Available: www.almaobservatory.org.
- [2] B. Billade "Design of Dual Polarization Sideband Separation Mixer for ALMA Band 5", Thesis for licentiate of engineering, ISBN/ISSN:1652-9103, Gothenburg 2009
- [3] ALMA Band 5 Workshop, "Science with ALMA Band 5 (163-211GHz)", Available: <http://web.oa-roma.inaf.it/meetings/AlmaBand5/Home.html>
- [4] Onsala Space Observatory webpage, Available: <http://www.oso.chalmers.se/~weather/index.html#humidity>
- [5] T.O. Klaassen, et. al., "Absorbing coatings and diffuse reflectors for the Herschel platform sub-millimetre spectrometers HIFI and PACS", 2002 IEEE Tenth Int. Conf. on Terahertz Electronics Proc. 2002.
- [6] A. R. Kerr, et. al., "Sideband Calibration of Millimeter-Wave Receivers", ALMA Memo #357, March 2001
- [7] G.H. Tan, "Band 5 Cartridge Technical Specifications", Doc. nr: FEND-40.02.05.00-001-A-SPE, 2005.
- [8] Lazareff, Mahieu, "Band 7 Cartridge Test Report Gain Saturation", Doc.: FEND-40.02.07.00-013-B-PRO, IRAM 2006.
- [9] O. Nyström, et. al., "A Vector Beam Measurement System for 211-275 GHz", Proc. EuCAP 2006, France, (ESA SP-626, October 2006) ISBN/ISSN: 92-9092-937-5.
- [10] TICRA, webpage available: <http://www.ticra.com/what-we-do/software-descriptions/grasp/>
- [11] University of Ireland, Maynooth, IRLAND.